Journal of
Polymer Materials

Tech Science Press

http://doi.org/10.32604/jpm.2026.087727

ARTICLE

Environmentally Sustainable Vitrimer Derived from Renewable Rosin: Shape Memory, Self-Healing Performance and Hydrothermal Degradation

Yanhe Wang[1], Ruiqin Deng[2] and Xinyan Yan[2,*]

[1]College of Resources and Environment, Huazhong Agricultural University, Wuhan, China
[2]School of Chemistry & Chemical Engineering, Yancheng Institute of Technology, Yancheng, China
*Corresponding Author: Xinyan Yan. Email: 18752008824@163.com

Received: 22 June 2026; Accepted: 29 July 2026; Published: 24 September 2026

ABSTRACT: To mitigate the environmental hazards of traditional petroleum thermosets and develop sustainable alternative materials, in this work, Dehydroabietylamine (DHAA), a renewable rosin derivative, was employed as the bio-based raw material to fabricate an environmentally benign vitrimer. Diglycidyl Dehydroabietylamine Epoxy Resin (DGDHAA) was first synthesized using DHAA and epichlorohydrin (ECH). The chemical structure of the synthesized DGDHAA was systematically characterized by FT-IR, ^{13}C NMR, and ^{1}H NMR techniques. Subsequently, a bio-based vitrimer (denoted as DGDHAA/ESO-MNA) was prepared through the epoxy-anhydride curing reaction, with DGDHAA as the matrix, epoxidized soybean oil (ESO) as the toughening modifier, and methyl nadic anhydride (MNA) as the curing agent, and triethanolamine (TEOA) in this study, served not only as a catalyst but also as a source of hydroxyl groups to promote dynamic hydroxy-ester bond exchange. To optimize the material properties, the effects of different epoxy/anhydride molar ratios on the thermal stability, dynamic mechanical properties, and tensile mechanical properties of the vitrimers were investigated. The prepared vitrimers exhibited good shape memory performance and self-healing capability. Importantly, the material could undergo hydrothermal degradation, achieving a 100% degradation rate at 190°C for 6 h, which further highlights its environmentally benign and sustainable characteristics.

KEYWORDS: Rosin derivative; vitrimer; shape memory; self-healing; hydrothermal degradation

1 Introduction

Polymer materials are broadly categorized into thermoplastics and thermosets. While thermoplastics exhibit good reprocess ability, they generally suffer from limited mechanical performance. In contrast, thermosetting polymers possess superior mechanical properties owing to their three-dimensional crosslinked network structures; however, once cured, they are difficult to degrade, recycle, or reprocess [1–4]. This not only leads to environmental pollution but also results in resource waste throughout their lifecycle—from production and use to end-of-life disposal.

The concept of vitrimer was first proposed by the French scientist Leibler [5]. As a novel category of materials, vitrimers are constructed by integrating dynamic covalent bonds into thermosetting polymer networks, and thus are classified as covalent adaptable networks (CANs) endowing the materials with excellent properties such as re-processability, recyclability, shape memory, and degradability. This innovative design addresses the long-standing drawbacks of traditional three-dimensionally crosslinked thermosets—including poor degradability, difficulty in recycling, environmental pollution, and resource waste [6–11]. By incorporating strong crosslinking sites of acid-base ionic pairs into dense hydrogen-bonding networks,

Jing et al. balanced the conflicting mechanical and dynamic performances of supramolecular polymers [12]. The as-prepared material allows real-time stiffness regulation through electrical heating and delivers a healing efficiency of 92% at 40°C. This finding verifies that hierarchically dynamic bonds can eliminate the inherent trade-off between mechanical strength and dynamic adaptability of polymers, providing a design guideline for multifunctional smart polymers. The Du Prez team from Ghent University in Belgium developed a new type of vitrimer based on non-isocyanate polyurethane (NIPU). They employed macromolecular amines to induce the ring-opening of multifunctional N-substituted eight-membered cyclic carbonates, integrating dynamic carbamate bonds into the NIPU network while embedding tertiary amines as internal catalytic sites. This advancement effectively overcomes the processability challenges faced by traditional polyurethanes [13]. The research group led by Zhang Wei at the University of Colorado in the United States has made remarkable contributions to the development of fully recyclable polyimine vitrimers [14,15]. They demonstrated that such composites can be rapidly formed and *in situ* repaired under mild conditions; moreover, nearly complete recovery of both the polyimide matrix and carbon fibers was achieved through chemical depolymerization in an acidic environment, with their original performance well retained. Guo [16] reported a facile method for the fabrication of dual dynamic cross-linked polymer complexes that simultaneously possess multiple remarkable mechanical properties and room-temperature self-heal ability by simply mixing polymers that have complementary interactions in solutions.

However, more than 98% of commercial epoxy resins worldwide are petroleum-based, relying heavily on feedstocks from the petrochemical industry [17,18]. For instance, the bisphenol A (BPA) used in BPA epoxy resins is entirely derived from fossil fuels. Moreover, BPA is known to exhibit reproductive toxicity [19–24]. With the gradual depletion of petroleum resources and growing environmental awareness, replacing petroleum-based chemicals with non-toxic, renewable alternatives has become an essential pathway toward sustainable and greener development. Bio-based epoxy resins, synthesized from continuously renewable raw materials, offer promising application prospects due to their advantages in carbon footprint reduction, molecular structural tunability, low toxicity, and environmental friendliness. Consequently, the adoption of bio-based epoxy resins as alternatives to conventional petroleum-based ones is steadily increasing [25,26]. In this regard, researchers have developed vitrimers derived from bio-based lignins and plant oils, thereby opening new avenues for green polymer chemistry [27–29].

Rosin, a natural resin derived chiefly from pine trees, consists predominantly of resin acids featuring a characteristic tricyclic phenanthrene skeleton. It benefits from natural renewability, high annual production, and low cost [30,31]. Among its major constituents is abietic-type acids, which can be chemically modified to yield a variety of derivatives. One of the most valuable derivatives is dehydroabietylamine (DHAA), produced through the reduction and structural rearrangement of dehydroabietic acid.

In this study, a bio-based epoxy resin, diglycidyl dehydroabietylamine (DGDHAA), synthesized from DHAA, was blended with flexible epoxidized soybean oil (ESO) to obtain a tunable matrix with balanced rigidity and toughness. Methyl nadic anhydride (MNA) was used as the curing agent, and triethanolamine (TEOA) in this study, a hydroxyl-amine compound, is incorporated as a catalytic co-curing agent into a typical DGDHAA/ESO-epoxy/MNA-anhydride curing system to form a TEOA-mediated covalent adaptable network. The hydroxyl groups and tertiary amine moiety of TEOA catalyze the curing process. As a multifunctional additive, TEOA not only acts as a catalyst to reduce the activation energy for network rearrangement at elevated temperatures but also provides hydroxyl groups facilitating dynamic hydroxy-ester bond exchange; meanwhile, the tertiary amine and regenerated hydroxyl groups within the crosslinked network further accelerate dynamic transesterification [32]. A vitrimer containing dynamic covalent bonds

was thus prepared, and its mechanical properties, self-healing ability, shape-memory performance, and degradability were systematically investigated.

2 Materials and Method

2.1 Materials

Dehydroabietylamine (DHAA, 98%, Xuancheng Jingrui New Materials Co., Ltd.), Epichlorohydrin (ECH, AR, Shanghai Yansu Technology Co., Ltd.), Tetrabutylammonium bromide (TBAB, 99%, Saan Chemical Technology (Shanghai) Co., Ltd.), Sodium hydroxide (NaOH, AR, Jiangsu Tongsheng Chemical Reagent Co., Ltd.), Magnesium sulfate anhydrous ($MgSO_4$, AR, Shanghai Pilot Chemical Corporation), Petroleum ether (PE, AR, Shanghai Lingfeng Chemical Reagent Co., Ltd.), Crystal violet (CV, 94%, Shanghai Yuanye Biotechnology Co., Ltd.), Acetic acid (HOA_C, AR, Anhui Tiandi High Purity Solvent Co., Ltd.), Perchloric acid ($HClO_4$, AR, Tianjin Dongfang Chemical Plant), Acetic anhydride (AR, Jiangsu Tongsheng Chemical Reagent Co., Ltd.), Tetraethylammonium bromide (TEAB, 97%, Shanghai Bide Pharmaceutical Technology Co., Ltd.), Trichloromethane ($CHCl_3$, 99.5%, Shanghai McLean Biochemical Technology Co., Ltd.), Potassium hydrogen phthalate (KHP, 99.95%, Yonghua Chemical Technology (Jiangsu) Co., Ltd.), Diglycidyl dehydroabietylamine epoxy resin (DGDHAA, Lab-made), Epoxidized soybean oil (ESO, AR, Shanghai McLean Biochemical Technology Co., Ltd.), Methyl nadic anhydride (MNA, 97%, Shanghai Haohong Biomedical Technology Co., Ltd.), Triethanolamine (TEOA, AR, Jiangsu Tongsheng Chemical Reagent Co., Ltd.), Toluene (PhMe, AR, China National Pharmaceutical Group Chemical Reagent Co., Ltd.), Absolute ethanol (EtOH, AR, Shanghai Lingfeng Chemical Reagent Co., Ltd.). All water used in the experiments was distilled water.

2.2 Preparation of Diglycidyl Dehydroabietylamine Epoxy Resin (DGDHAA)

The DGDHAA was prepared from dehydroabietylamine (DHAA) and epichlorohydrin. The synthesis route is shown in Fig. 1.

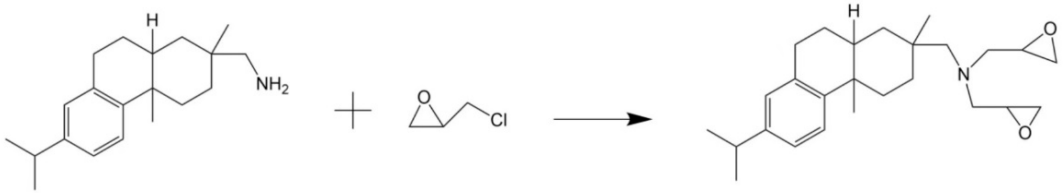

Figure 1: Synthetic route of DGDHAA.

To ensure high conversion and obtain a high-purity monomer product, the reaction conditions and purification procedures in this study were carefully controlled. The detailed synthesis steps are as follows:

Dehydroabietylamine (57 g) and an excess of epichlorohydrin (223.2 g) were mixed, followed by the addition of 10 mL of deionized water. The mixture was then placed in a constant-temperature oil bath at 45°C. To promote complete reaction of the sterically hindered dehydroabietylamine and suppress side reactions, the system was maintained at this temperature for 150 h. Subsequently, tetrabutylammonium bromide (TBAB) was introduced as a phase-transfer catalyst to enhance mass transfer between the aqueous and organic phases. A 15 wt% NaOH aqueous solution was added dropwise, and the mixture was stirred continuously for 3 h at the same temperature. This step facilitated the elimination of hydrogen chloride from the intermediate under alkaline conditions, thereby promoting dehydrochlorination and the formation of terminal epoxy groups.

After the reaction, the crude product was worked up to remove by-products and impurities. Precipitated inorganic salts were first removed by vacuum filtration. The collected filtrate was treated with an appropriate amount of anhydrous magnesium sulfate, left to stand to adsorb residual water, and then filtered to remove the drying agent. The resulting organic phase was extracted and washed with petroleum ether, which selectively dissolved nonpolar components, thereby separating unreacted starting materials and low-polarity impurities. Finally, the purified product was dried to constant weight in a vacuum oven to afford the target compound DGDHAA.

2.3 Preparation of Bio-Based Vitrimer—DGDHAA/ESO-MNA

DGDHAA/ESO-MNA was prepared with DGDHAA as raw material, ESO, MNA and TEOA in different proportions.

In order to ensure that the final cured product has a dense crosslinking network and excellent comprehensive properties, the blending ratio, defoaming process and curing procedure of the resin system are carefully designed and finely regulated in this section. In all formulations, the mass ratio of rigid bio-based monomer DGDHAA to flexible ESO is strictly fixed at 1:1, in order to achieve an ideal balance between the rigidity and toughness of the material. The curing formula refers to Table 1. The amount of TEOA used in the formulation accounted for 0.38 wt% of the total mass of all raw materials.

Table 1: Curing formulation of the DGDHAA/ESO-MNA system.

Sample	DGDHAA (g)	ESO (g)	MNA (g)
DGDHAA/ESO-MNA 0.6	1	1	1.0476
DGDHAA/ESO-MNA 0.7	1	1	1.2220
DGDHAA/ESO-MNA 0.8	1	1	1.3968
DGDHAA/ESO-MNA 0.9	1	1	1.5714

2.4 Characterizations

Fourier transform infrared (FTIR) spectroscopy was performed on a Nicolet iS20 spectrometer using the KBr pellet method. The spectra were recorded over the wavenumber range of 500–4000 cm^{-1}. ^{1}H NMR and ^{13}C NMR spectra were recorded on an Avance Neo 500 MHz NMR spectrometer using $CDCl_3$ as the solvent. Epoxy Value was measured by perchloric acid method. Dynamic thermomechanical analysis (DMA) was conducted on a TA Instruments Q800 analyzer under the following conditions: an oscillation frequency of 1 Hz, a temperature range from 25 to 200°C, and a heating rate of 3°C/min. Stress relaxation tests were performed at 130°C with an oscillation frequency of 1 Hz and a strain of 2%. Thermogravimetric–differential scanning calorimetry (TG–DSC) was performed by STA 449C3/G under a nitrogen atmosphere from room temperature to 800°C at a heating rate of 10°C/min. An electronic universal testing machine (UTM 6503 SUNS Technology Stock Co., Ltd.) was used to measure tensile properties of the dogbone-shaped samples according to ASTM D638 with 25 mm/min crosshead speed. Molecular weight distribution curves and relative values of number-average (Mn) and weight-average (Mw) molecular weight of the degradation products were determined by Gel permeation chromatography (GPC). GPC was performed on a Waters e2695 system equipped with a Waters 2414 refractive index detector at room temperature. Separation was achieved using a series of Waters Styragel® columns (HR5 + HR4 + HR3, 300 × 7.8 mm each) coupled with a guard column compatible with THF as the mobile phase at a flow rate of 1.0 mL/min.

2.5 Epoxy Value Titration of DGDHAA

Epoxy value is an important parameter to characterize epoxy resin, which is defined as the equivalent number of epoxy groups per 100 g of resin (that is, the number of moles of epoxy groups). In practical application, epoxy value is also the basic basis for calculating the amount of curing agent, which has important reference significance for formula design.

The structure of DGDHAA contains tertiary amine group, so the epoxy value cannot be determined by hydrochloric acid acetone method, because the tertiary amine group will consume hydrochloric acid, resulting in small measurement results. Therefore, perchloric acid method should be used to determine the epoxy value of the resin containing tertiary amine group.

Experimental steps and calculation for determination of epoxy value by perchloric acid method:

(1) Preparation of solution

Preparation of crystal violet indicator:

Weigh 0.5 g of crystal violet, add 100 mL of acetic acid, put it in a volumetric flask, shake well, and cover it for use;

Prepare potassium hydrogen phthalate solution:

Weigh 0.2 g of potassium hydrogen phthalate (dry in a 120°C oven for 12 h before use), add 10 mL of acetic acid, shake well in a volumetric flask, and cover for use; The solution needs to be prepared into three groups of parallel control group and blank control group without potassium hydrogen phthalate (excluding the influence of other interference factors on the experimental results).

Prepare perchloric acid acetic acid solution:

Weigh 300 mL of acetic acid into a 500 mL beaker, add 8.5 mL of 70% perchloric acid aqueous solution, add 20 mL of acetic anhydride, transfer the solution to a 1000 mL volumetric flask, dilute to 1 L with acetic acid and shake well.

Calibration perchloric acid acetic acid solution:

After the solution is prepared, the perchloric acid solution is calibrated with potassium hydrogen phthalate solution using crystal violet as the indicator. Slowly add perchloric acid acetic acid solution to potassium hydrogen phthalate solution containing crystal violet indicator until the color of the solution changes from purple to blue and does not fade for 30 s. Perchloric acid concentration (mol/L) is calculated as follows:

$$N = m/(V \times 0.20422)$$

where

m is the mass of potassium hydrogen phthalate (g);
V is the volume of perchloric acid solution consumed by titration (mL);
0.20422 is the molar mass of potassium hydrogen phthalate (g/mmol).

(2) Preparation of tetraethylammonium bromide acetic acid solution

Dissolve 100 g of tetraethylammonium bromide in 400 mL of acetic acid and stir constantly to fully dissolve it.

(3) Epoxy value measurement

① Weigh three portions of 0.3 g DGDHAA into three conical flasks and label them for parallel test. Add 10 mL trichloromethane each and shake the sample to dissolve it;

② Add 20 mL glacial acetic acid to each of the three samples, and accurately add 10 mL tetraethylammonium bromide acetic acid solution to each sample using a pipette. Drop 4–6 drops of crystal violet indicator into each sample to indicate the titration end point. Shake each sample sufficiently to mix it evenly. Then immediately titrate with perchloric acid acetic acid solution of known concentration in turn until a stable green color (no fading within 30 s) is obtained, which is regarded as the end of titration. Record the volume V_1 of the perchloric acid solution used.

③ Three groups of blank parallel test control group were conducted respectively: the average volume of perchloric acid solution used for blank test without adding sample was V_0. Then the epoxy value of the epoxy resin was calculated as follows:

$$EPV = (V_1 - V_0)M/10W$$

where

V_1 is the volume of perchloric acid used for the sample (mL),
V_0 is the average volume from blank titrations (mL),
M is the concentration of perchloric acid (mol/L),
W is the sample weight (g).

2.6 Gel Content and Swelling Ratio Testing

The gel content and swelling ratio are tested according to ASTM D2765. About 2.0 g of dry sample (W_1) is wrapped with filter paper and put into Soxhlet extractor for refluxing extraction with toluene for 12 h. After taking it out, the solvent on the surface of the swollen sample is absorbed with filter paper, and the mass of the swollen sample (W_g) is weighed, dried in an oven, and weighed after the mass is constant (W_2). The gel content and swelling ratio are calculated according to the following formula:

$$\text{Gel content (\%)} = W_2/W_1 \times 100\%$$

$$\text{Swelling ratio} = 1 + \rho_{polymer}(W_g - W_2)/\rho_{solvent}W_2$$

3 Results and Discussion

3.1 Characterization of DHAA and DGDHAA

The structure of DGDHAA synthesized from DHAA and epichlorohydrin was effectively characterized by FT-IR spectroscopy. Fig. 2 compares the FT-IR spectra of DHAA and DGDHAA. Both spectra exhibit strong absorption bands in the 2800–3000 cm^{-1} region, with nearly identical peak shapes and positions, indicating that the phenanthrene-ring skeleton of the rosin-based structure remains stable during the reaction with epichlorohydrin, without significant structural alteration. In the spectrum of DGDHAA, a new absorption peak appears near 968 cm^{-1} (marked with a dashed box in the figure), which can be assigned to the characteristic asymmetric stretching vibration of the epoxy group, confirming the successful introduction of epoxy functional groups into the molecular structure.

The structure of DGDHAA synthesized from DHAA and epichlorohydrin was further confirmed by ^1H NMR spectroscopy. Fig. 3A compares the ^1H NMR spectra of DHAA and DGDHAA. The proton signals of the aromatic ring (δ 6.8–7.2) and the rosin-tricyclic skeleton (δ 0.8–2.3) remained essentially unchanged after the reaction, indicating that the rigid tricyclic phenanthrene skeleton of DHAA remained stable throughout the synthesis. In contrast to the spectrum of DHAA, that of DGDHAA exhibited two new sets

of multiplets at δ 2.5 and δ 2.7 (labeled as peaks a and b in the figure), corresponding to the characteristic proton signals of the epoxy group. The chemical shifts, splitting patterns, and proton integrals of these new signals are fully consistent with the theoretical ^{1}H NMR profile of DGDHAA, confirming the successful introduction of the epoxy functionality.

The molecular skeleton and functional group carbon sites of DHAA and DGDHAA were further confirmed by ^{13}C NMR. Fig. 3B shows the ^{13}C NMR spectra of DHAA and DGDHAA. By comparing the upper and lower spectra, it can be found that the aromatic ring carbon signal in the range of δ 120–150 and the rosin ring skeleton carbon signal in the range of δ 15–50 show a high degree of coincidence before and after the reaction, which indicates that the rigid tricyclic phenanthrene skeleton of DHAA maintains excellent stability during the epoxidation reaction without side reactions. Comparing the spectra of raw material DHAA, it can be seen that the product DGDHAA exhibits two new characteristic signals (a, b peaks in DGDHAA) at δ 62 and δ 68, which are the characteristic peaks of epoxy group in ^{13}C NMR spectra and highly coincide with the theoretical range of carbon chemical shift of epoxy functional group. In addition, the chemical shifts, peak shapes and relative intensities of the remaining carbon signals in the DGDHAA spectrum are highly matched with the target molecules, and no obvious impurity peaks were observed, indicating that the product has high purity and regular molecular structure.

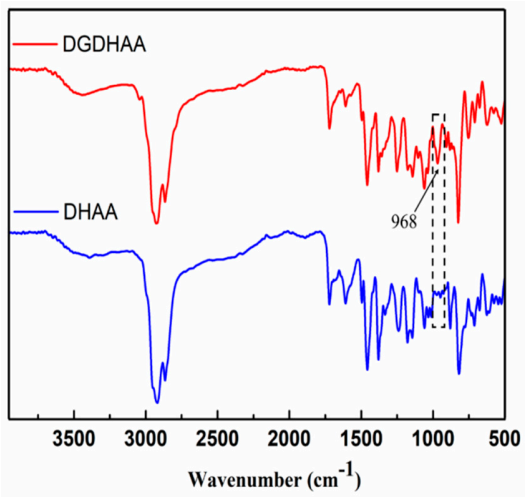

Figure 2: FT-IR of DHAA and DGDHAA.

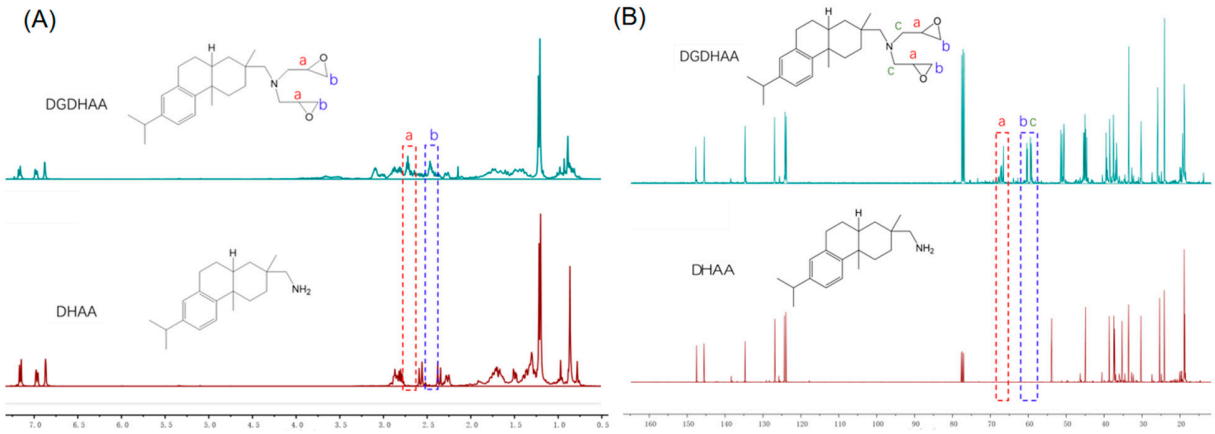

Figure 3: (**A**) ^{1}H NMR spectra of DHAA and DGDHAA; (**B**) ^{13}C NMR spectra of DHAA and DGDHAA.

The results of FT-IR, ^{1}H NMR and ^{13}C NMR can be used to judge the chemical structure of DGDHAA. The new characteristic absorption peak of epoxy group at 968 cm^{-1} in the infrared spectrum preliminarily confirmed the successful transformation of functional groups; the new characteristic resonance signals in the hydrogen nuclear magnetic resonance spectrum (δ 2.5–2.8) and carbon spectrum (δ 58–70) further located the access sites of epoxy groups. All spectra showed that the rigid tricyclic phenanthrene skeleton of dehydroabietylamine remained the same before and after the reaction. The expected bio-based epoxy resin prepolymer, DGDHAA, was successfully synthesized. The epoxy value of DGDHAA measured by the perchloric acid method is 0.47 mol/100 g, and the theoretical value is 0.49 mol/100 g, reaching 95.91% of the theoretical value.

3.2 Performance Study of DGDHAA/ESO-MNA

3.2.1 Thermal Stability

The DGDHAA/ESO-MNA system with different proportions of epoxy and anhydride was analyzed by thermogravimetry. The curve of weight loss rate with temperature is shown in Fig. 4A. Fig. 4B presents the derivative thermogravimetry (DTG) curves of the DGDHAA/ESO-MNA systems with different epoxy-to-anhydride ratios. In the temperature range of 150–280°C, DGDHAA/ESO-MNA 0.6 and DGDHAA/ESO-MNA 0.7 exhibited no distinct weight-loss peak or only a very weak shoulder peak, indicating a relatively denser cross-linked network. In contrast, as the MNA ratio increased, a pronounced broad peak appeared in the same range for DGDHAA/ESO-MNA 0.8 and DGDHAA/ESO-MNA 0.9, and its area expanded considerably with higher MNA content. The excess anhydride in DGDHAA/ESO-MNA 0.9 likely did not fully participate in the three-dimensional network, or formed thermodynamically less-stable ester bonds due to localized over-cross-linking. Moreover, residual unreacted MNA monomer may be present, collectively reducing the thermal stability and leading to premature degradation at lower temperatures.

The most pronounced valley in the DTG curves, located between 300 and 400°C, corresponds to the maximum thermal-degradation rate, and its position on the temperature axis defines the peak degradation temperature (T_{max}). DGDHAA/ESO-MNA 0.6 displayed the sharpest main peak with $T_{max} \approx 340$°C, reflecting a highly uniform cross-linked network in which chemical bonds break almost simultaneously upon reaching the critical temperature. As the MNA ratio increased from 0.6 to 0.9, the main degradation peak shifted noticeably to lower temperatures; for DGDHAA/ESO-MNA 0.9, T_{max} decreased to about 320°C. The higher MNA content introduced more rigid structural motifs and increased steric hindrance, resulting in a heterogeneous network. Upon heating, the weakly cross-linked regions degraded first, followed by the more stable zones, which slightly lowered the overall thermal stability of the material. Overall, this class of materials exhibits good thermal stability.

3.2.2 Dynamic Mechanical Analysis

The temperature-dependent tan δ curves of the DGDHAA/ESO-MNA systems with different epoxy-to-anhydride molar ratios were shown in Fig. 4C. All samples exhibited a single tan δ peak, indicating good compatibility between DGDHAA and ESO in the cured network and the absence of macroscopic phase separation. The peak temperature of tan δ corresponds to the glass-transition temperature (T_g), which reflects the cross-linking density of the system. As the epoxy/anhydride ratio varied, T_g initially increased from 68.87°C to a maximum of 72.72°C, and then slightly decreased to 71.77°C upon further increase in anhydride content. The highest T_g was achieved at a molar ratio of 1:0.7, suggesting that under this formulation, the reaction between epoxy and anhydride groups proceeds more completely, yielding a

greater number of effective cross-linking points, a denser network structure, and consequently improved heat resistance of the material.

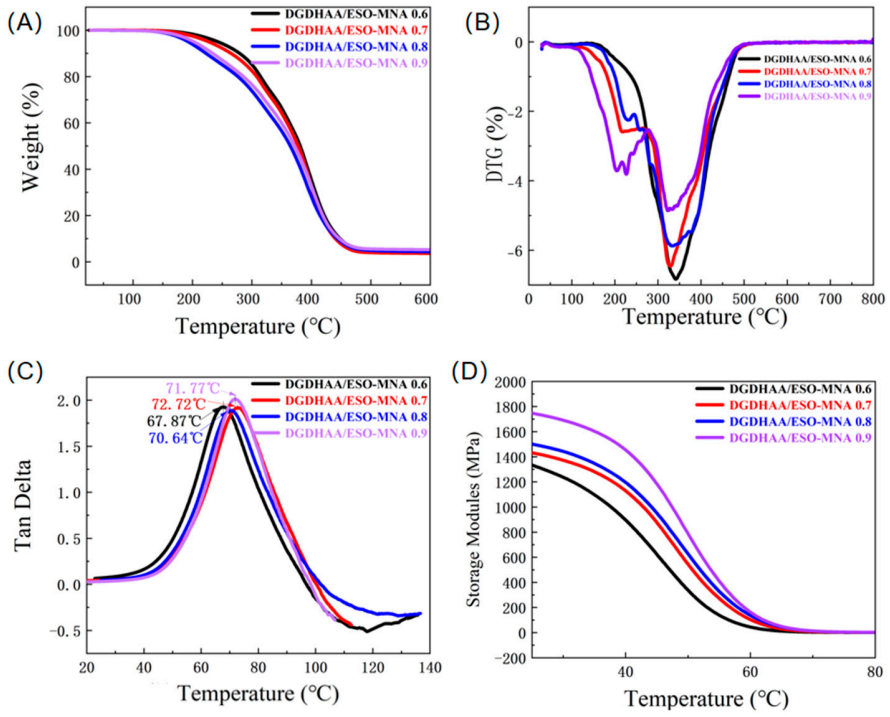

Figure 4: (**A**) thermogravimetric curves of DGDHAA/ESO-MNA; (**B**) DTG curve of DGDHAA/ESO-MNA; (**C**) curves showing the relationship between tanδ and temperature; (**D**) curves depicting the relationship between modulus and temperature.

The storage modulus curves of DGDHAA/ESO-MNA system under different epoxy/anhydride molar ratios were shown in Fig. 4D. At ambient temperature, with the increase of epoxy/anhydride molar ratio from 1:0.6 to 1:0.9, the storage modulus also increased, indicating that increasing the amount of anhydride is helpful to promote the ring opening esterification reaction and increase the network crosslinking node. The apparent crosslinking density was the highest when the ratio was 1:0.9, while the T_g peak appeared at 1:0.7, and the two were not completely synchronized. This phenomenon may be related to the failure of some components in the excess anhydride to effectively participate in the construction of three-dimensional network, and the rigid structure provided by it has limited improvement on T_g.

According to the analysis results of Tan δ and storage modulus, the epoxy/anhydride molar ratio of 1:0.7 achieved a reasonable balance between the degree of crosslinking and the perfection of network structure.

3.2.3 Mechanical Properties

Fig. 5 shows the stress-strain curves of DGDHAA/ESO-MNA system under different epoxy/anhydride molar ratios. It can be seen from the figure that the tensile strength of the system increases first and then decreases with the increase of MNA content. When the molar ratio increases from 1:0.6 to 1:0.7, the tensile strength increases from 21.36 ± 3.33 MPa to 23.19 ± 3.66 MPa. At an epoxy ratio of 1:0.7, the reaction degree of epoxy group and anhydride functional group is relatively sufficient, and the network crosslinking density is high, which is conducive to the enhancement of mechanical properties. When the amount of anhydride was further increased, the tensile strength did not increase, but decreased to 16.41 ± 3.85 MPa at a higher

ratio. This change may be related to the introduction of more rigid ring structures by excessive MNA. The excessive content of rigid components reduces the flexibility of the network, increases the brittleness of the material, and thus significantly reduces the tensile strength.

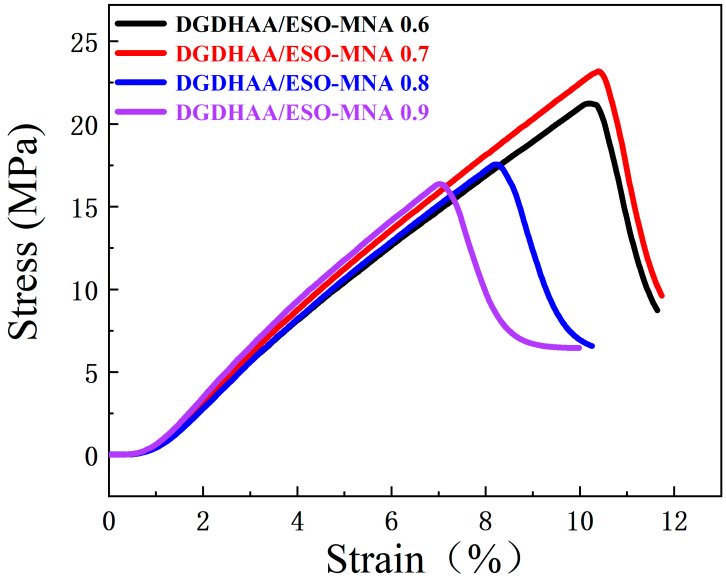

Figure 5: The stress-strain curves of DGDHAA/ESO-MNA.

3.2.4 Gel Content and Swelling Ratio

As shown in Fig. 6, gel content and swelling ratio of DGDHAA/ESO-MNA curing system under different proportions. Gel content and swelling ratio are important macro indicators to evaluate the crosslinking density and network integrity of thermosetting resin. The test results show that with the increase of the ratio of the system from 0.6 to 0.9, the physical properties of the system show a trend of first increasing and then decreasing (gel content from 75.83% → 79.80% → 71.10% → 74.15%, swelling rate from 1.100 → 1.046 → 1.137 → 1.243). When the ratio is 0.7, the gel content of the system reaches the maximum value of 79.80%, which shows that under this ratio, the reaction between epoxy and anhydride is the most sufficient, thus forming a three-dimensional network with the densest cross-linking points and the densest structure. When the molar ratio of epoxy to anhydride deviates from 1:0.7 (such as 1:0.6, 1:0.8 or 1:0.9), the gel content decreases significantly. This is mainly because excessive epoxy groups or curing agents cannot fully participate in the crosslinking reaction, forming unreacted small molecules in the network, reducing the density of the network, making it easier for solvent molecules to penetrate and open the polymer network. DGDHAA/ESO-MNA 0.7 system showed the highest T_g (72.72°C) and good thermal stability because its highest crosslinking density limited the thermal movement of polymer segments to the greatest extent. In conclusion, DGDHAA/ESO-MNA 0.7 represents the optimal formulation for achieving the most favorable cross-linked network structure. Therefore, this composition was selected for the further investigations.

3.2.5 Stress Relaxation Performance

Stress relaxation is the key thermodynamic behavior to evaluate the dynamic covalent bond exchange ability of vitrimer materials. As shown in Fig. 7, the stress relaxation behavior of different proportion systems at 130°C was tested. The DGDHAA/ESO-MNA 0.7 sample exhibited moderate stress relaxation at 130°C. Its normalized relaxation modulus (G/G_0) gradually decreased from approximately 0.99 to 0.61 over

the test duration, and the relaxation time was about 30.22 s, which verifies the dynamic transesterification of hydroxyl–ester bonds within the covalent adaptable network.

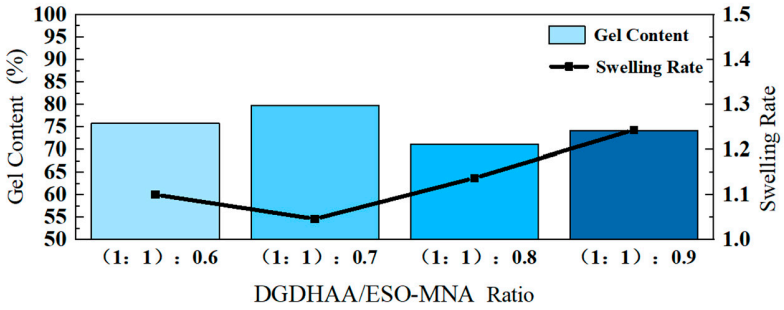

Figure 6: Gel content and swelling ratio of DGDHAA/ESO-MNA.

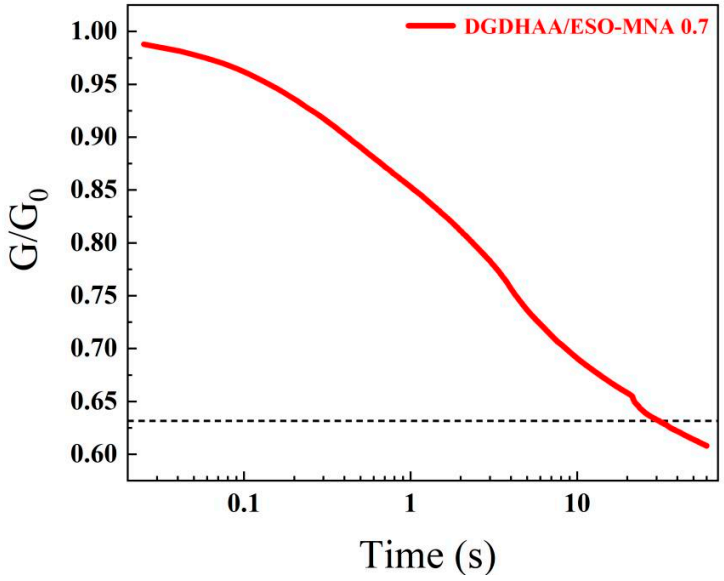

Figure 7: Stress relaxation of DGDHAA/ESO-MNA 0.7.

3.2.6 Self-healing Performance

Based on the stress relaxation test, the self-healing properties of DGDHAA/ESO-MNA 0.7 samples were investigated. As shown in Fig. 8, cross-shaped scratches were made on the sample surface using a blade on the surface of the sample, and conduct constant temperature treatment at 90°C and 130°C for 1 h respectively, and observe the changes of scratch morphology through an optical microscope. For a scratch with an initial width of 20 μm, after heating at 90°C for 1 h, the scratch width decreased to 10 μm, corresponding to a self-healing efficiency of 50% (calculated as the reduction in scratch width relative to the initial width). For a scratch with an initial width of 32 μm, after heating at 130°C for 1 h, the scratch width decreased to 8 μm, corresponding to a self-healing efficiency of 75%. These results demonstrate that the material exhibits clear temperature-dependent self-healing behavior, with higher healing efficiency achieved at elevated temperatures due to accelerated dynamic transesterification. At temperatures higher than the glass transition temperature, the material undergoes rapid transesterification. Through the fracture and recombination of covalent bonds at the scratch, the deep topological network rearrangement occurred,

and finally the scratch repair was realized. These results indicate that the bio-based epoxy vitrimer system has certain self-healing ability.

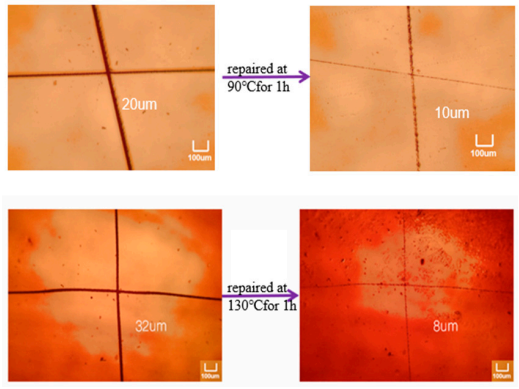

Figure 8: Self-healing of DGDHAA/ESO-MNA0.7.

3.2.7 Shape Memory Performance

The crosslinked epoxy-anhydride network exhibits conventional thermally induced shape-memory properties. When the ambient temperature exceeds the glass-transition temperature (T_g), polymer chains acquire sufficient mobility to enable elastic deformation of the network under external force. As illustrated in Fig. 9A, the film sample can be deformed into a temporary shape (e.g., an "S-shape") upon the application of external force, followed by rapid cooling to room temperature. The material stably maintains this temporary shape even after removal of the external load. Upon reheating above T_g, the conformational entropy of polymer chains drives spontaneous recovery to the initial permanent shape. Although dynamic transesterification takes place within the network, it is not the primary driving force for temporary shape recovery. These dynamic covalent bonds preserve the structural integrity of the crosslinked network during cyclic deformation. Consequently, the shape-fixity and shape-recovery ratios show negligible degradation over multiple cycles, verifying the excellent shape-memory performance of the vitrimer.

Whereas conventional shape-memory materials can only switch between a programmed temporary shape and a fixed permanent shape—which limits their adaptability in complex application scenarios—the dynamic covalent bonds in the DGDHAA/ESO-MNA 0.7 system enable reversible shape reconfiguration, offering greater flexibility in practical use.

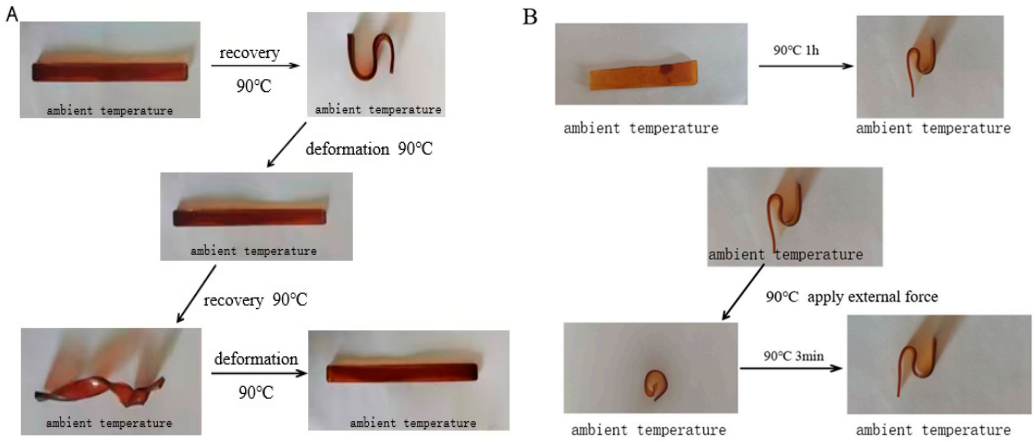

Figure 9: (**A**) shape memory of DGDHAA/ESO-MNA 0.7; (**B**) shape change of DGDHAA/ESO-MNA 0.7.

Fig. 10 shows the shape recovery process of DGDHAA/ESO-MNA 0.7 sample at different temperatures. At 90°C, the time required for the sample to completely return from the temporary twisted state to the initial rectangular shape is 4 min; When the temperature was increased to 130°C and 150°C, the recovery time was significantly shortened to 80 s and 50 s; when the temperature reached 190°C, the recovery time of the sample was the shortest, only 35 s. Temperature plays a key role in accelerating the dynamic transesterification reaction. As the temperature increases, the exchange rate of dynamic covalent bonds rises significantly, leading to faster network rearrangement. Consequently, the shape recovery of the material is noticeably shortened at elevated temperatures. Compared with the SMA-SMP mechanical composite structure proposed by Chen et al., which only achieves single bending deformation with fixed permanent shape and no self-healing capability, the rosin-based vitrimer in this study can repeatedly reshape its permanent configuration and realize complex deformations via dynamic covalent bonds, while possessing self-healing performance [33].

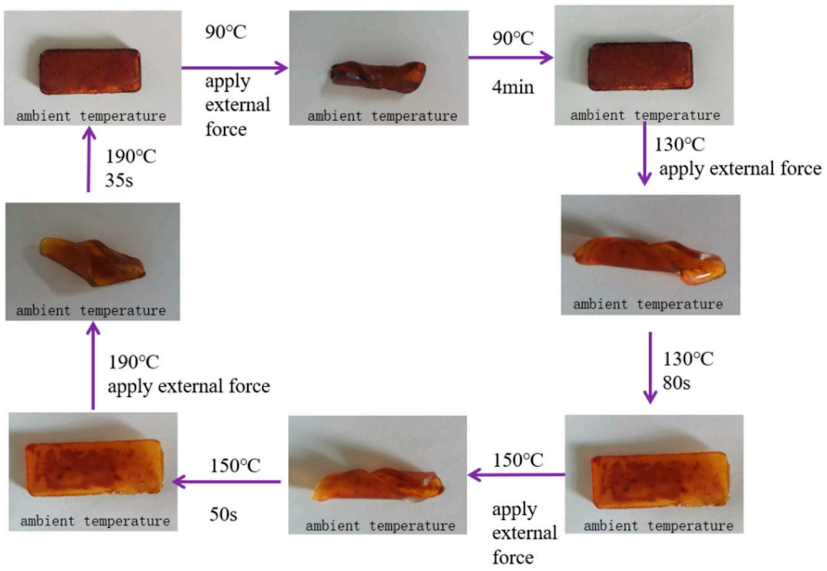

Figure 10: Shape memory of DGDHAA/ESO-MNA 0.7 at different temperatures.

3.2.8 Degradation Performance

Chemical recovery refers to the process of polymer decomposition into monomer or oligomer through chemical reaction. Because of the permanent network structure of highly crosslinked epoxy thermosetting resin, the recycling of waste epoxy thermosetting resin has always been a difficulty in the field of polymer science. Traditional chemical recovery not only consumes a lot of energy, but also is often accompanied by secondary environmental pollution. In this study, the dynamic covalent bond was used to endow the bio-based vitrimer with chemical instability at high temperature, so as to realize its efficient chemical recovery.

Compared with the current green and environmentally friendly chemical recovery method alcoholysis (which requires excessive consumption of ethanol or ethylene glycol) [34], this study adopted a cheaper and more environmentally friendly recovery path: using water as the reaction medium, the cured DGDHAA/ESO-MNA 0.7 sample was placed in a high-pressure reactor (solid content of 5 wt%) without catalyst, and reacted at constant temperature for 6 h. The results showed that the degradation product was soluble in ethanol, while the undegraded part was insoluble. The undegraded part was washed with ethanol, dried and weighed. The degradation rates at 120°C, 140°C, 160°C, 180°C and 190°C were 4.39%, 56.37%, 69.37%, 76.10% and 100%,

respectively, as shown in Fig. 11A. This non catalytic recovery scheme based on hydrothermal environment not only reduces the cost, but also embodies the concept of green environmental protection.

In order to further explore the degradation degree of DGDHAA/ESO-MNA 0.7 system in aqueous environment, gel permeation chromatography (GPC) was used to characterize the products after complete degradation to small molecules. The GPC curve in Fig. 11B shows that the retention time of elution peak of degradation products is mainly around 18.461, and the long retention time proves that the crosslinked polymer network was degraded into low-molecular-weight oligomers or monomers. According to the data analysis in Table 2, the weight average molecular weight of the degradation product is significantly reduced, which proves that the hydrothermal reaction can effectively decompose the polymer. Zhou et al. reported a thermally stimulated supramolecular cellulosic bioplastic that relies on natural microbial degradation in soil, which takes 55 days for complete decomposition and exhibits poor recyclability of raw materials. In contrast, the rosin-based vitrimer can be fully degraded in pure water without any external catalysts. This work provides a simpler and more sustainable strategy for the degradation and recycling of thermosetting vitrimers [35].

Table 2: Analysis of the average weight-average molecular weight of degradation products.

Peak#	Retention Time (min)	Peak Tip Molecular Weight (g/mol)	Number Average Molecular Weight (g/mol)	Weight Average Molecular Weight (g/mol)	Z Average Molecular Weight (g/mol)	Z+1 Average Molecular Weight (g/mol)	Polydispersity
1	18.461	403	227	610	1374	2479	2.687225

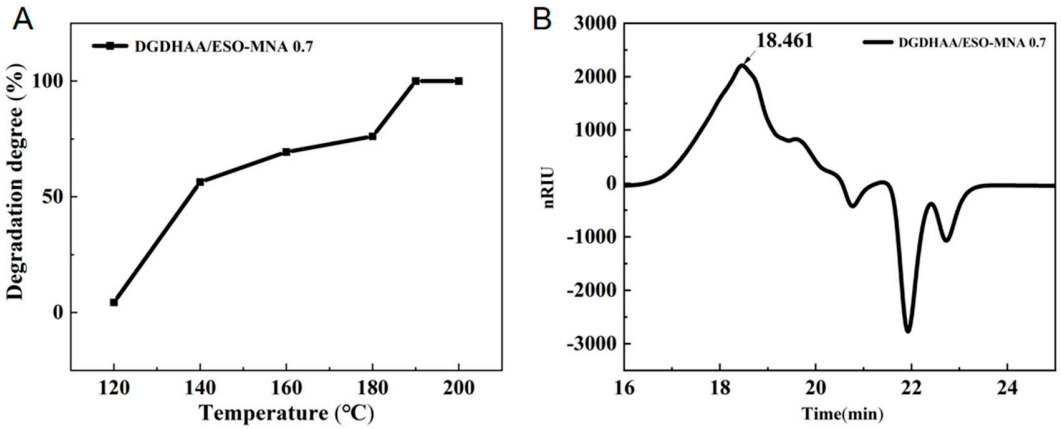

Figure 11: (**A**) relationship diagram of the effect of temperature on degradation rate; (**B**) gel permeation chromatogram (GPC chart).

4 Conclusion

In this work, a fully bio-based vitrimer with a covalent adaptable network was developed from renewable rosin-derived DGDHAA and ESO, cured with MNA at varied stoichiometries. TEOA was employed as a co-curing agent, utilizing its tertiary amine group to catalyze the epoxy–anhydride reaction autocatalytically, thereby eliminating the need for external catalysts and avoiding potential contamination from catalyst residues. The mechanical and thermal properties of the vitrimer were effectively tuned by the epoxy/anhydride ratio. A denser cross-linked network and enhanced rigidity were achieved with higher anhydride content, leading to an increase in the glass-transition temperature (T_g) and tensile strength. The optimal formulation, with an epoxy/anhydride molar ratio of 1:0.7, exhibited a balanced strength–

toughness profile and the highest tensile performance. Notably, the dynamic transesterification within the network endowed the material with repeatable shape memory, efficient self-healing, and closed-loop recyclability. More importantly, the vitrimer could be completely degraded in aqueous media at 190°C within 6 h, converting into reusable oligomers and thereby establishing a sustainable end-of-life pathway. This study demonstrates a green and catalyst-free strategy for fabricating high-performance vitrimers from renewable resources, highlighting their potential in designing environmentally benign, circular materials.

Acknowledgement: Not applicable.

Funding Statement: This research was financially supported by grants from Financial supports from Funding for School-level Research Projects of Yancheng Institute of Technology, China (xjr2022015).

Author Contributions: Data collection: Yanhe Wang; Analysis and interpretation of result: Ruiqin Deng; Draft manuscript preparation: Xinyan Yan. All authors reviewed and approved the final version of the manuscript.

Availability of Data and Materials: The datasets used and analyzed during the current study freely available from the corresponding author on reasonable request.

Ethics Approval: Not applicable.

Conflicts of Interest: The authors declare no conflicts of interest.

References

1. Kazemi M, Kabir SF, Fini EH. State of the art in recycling waste thermoplastics and thermosets and their applications in construction. Resour Conserv Recycl. 2021;174:105776. [CrossRef].
2. Sun L, Huang H, Guan Q, Yang L, Zhang L, Hu B, et al. Cooperative chemical coupling and physical lubrication effects construct highly dynamic ionic covalent adaptable network for high-performance wearable electronics. CCS Chem. 2023;5(5):1096–107. [CrossRef].
3. Wang S, Li B, Zheng J, Surat'man NEB, Wu J, Wang N, et al. Nanotechnology in covalent adaptable networks: From nanocomposites to surface patterning. ACS Mater Lett. 2023;5(2):608–28. [CrossRef].
4. Zhao W, Feng Z, Liang Z, Lv Y, Xiang F, Xiong C, et al. Vitrimer-cellulose paper composites: A new class of strong, smart, green, and sustainable materials. ACS Appl Mater Interfaces. 2019;11(39):36090–9. [CrossRef].
5. Montarnal D, Capelot M, Tournilhac F, Leibler L. Silica-Like Malleable Materials from Permanent Organic Networks. Science. 2011;334(6058):965–8. [CrossRef].
6. Schoustra SK, Dijksman JA, Zuilhof H, Smulders MMJ. Molecular control over vitrimer-like mechanics—Tuneable dynamic motifs based on the Hammett equation in polyimine materials. Chem Sci. 2020;12(1):293–302. [CrossRef].
7. Hayashi M. Implantation of recyclability and healability into cross-linked commercial polymers by applying the vitrimer concept. Polymers. 2020;12(6):1322. [CrossRef].
8. Anagwu FI, Thakur VK, Skordos AA. High-performance vitrimeric benzoxazines for sustainable advanced materials: Design, synthesis, and applications. Macro Mater Eng. 2023;308(4):2200534. [CrossRef].
9. Bergoglio M, Reisinger D, Schlögl S, Griesser T, Sangermano M. Sustainable bio-based UV-cured epoxy vitrimer from *Castor* Oil. Polymers. 2023;15(4):1024. [CrossRef].
10. Alabiso W, Schlögl S. The impact of vitrimers on the industry of the future: Chemistry, properties and sustainable forward-looking applications. Polymers. 2020;12(8):1660. [CrossRef].
11. Sharma H, Rana S, Singh P, Hayashi M, Binder WH, Rossegger E, et al. Self-healable fiber-reinforced vitrimer composites: Overview and future prospects. RSC Adv. 2022;12(50):32569–82. [CrossRef].
12. Jing J, Yao B, Sun W, Chen J, Xu J, Fu J. Ultra-tough, yet rigid and healable supramolecular polymers with variable stiffness for multimodal actuators. Angew Chem Int Ed. 2024;63(42):e202410693. [CrossRef].
13. Hernández A, Houck HA, Elizalde F, Guerre M, Sardon H, Du Prez FE. Internal catalysis on the opposite side of the fence in non-isocyanate polyurethane covalent adaptable networks. Eur Polym J. 2022;168:111100. [CrossRef].

14. Whiteley JM, Taynton P, Zhang W, Lee SH. Ultra-thin solid-state Li-Ion electrolyte membrane facilitated by a self-healing polymer matrix. Adv Mater. 2015;27(43):6922–7. [CrossRef].
15. Taynton P, Yu K, Shoemaker RK, Jin Y, Qi HJ, Zhang W. Heat- or water-driven malleability in a highly recyclable covalent network polymer. Adv Mater. 2014;26(23):3938–42. [CrossRef].
16. Guo H, Fang X, Zhang L, Sun J. Facile fabrication of room-temperature self-healing, mechanically robust, highly stretchable, and tough polymers using dual dynamic cross-linked polymer complexes. ACS Appl Mater Interfaces. 2019;11(36):33356–63. [CrossRef].
17. Ying J, Zhang Y, Chen J, Li SN, Han J, Wang Y, et al. Facile synthesis of phosphorus-free biobased epoxy resin with exceptional flame retardancy, mechanical properties, and heat resistance. ACS Appl Polym Mater. 2023;5(11):9445–55. [CrossRef].
18. Mashouf Roudsari G, Mohanty AK, Misra M. Green approaches to engineer tough biobased epoxies: A review. ACS Sustain Chem Eng. 2017;5(11):9528–41. [CrossRef].
19. Nikafshar S, Wang J, Dunne K, Sangthonganotai P, Nejad M. Choosing the right lignin to fully replace bisphenol A in epoxy resin formulation. ChemSusChem. 2021;14(4):1184–95. [CrossRef].
20. Karlsson I, Ponting DJ, Ortega MA, Niklasson IB, Ndreu L, Stéen EJL, et al. Nature-derived epoxy resin monomers with reduced sensitizing Capacity—Isosorbide-based bis-epoxides. Chem Res Toxicol. 2023;36(2):281–90. [CrossRef].
21. Liu SH, Zhang XQ, Liu JH, Lei CH, Dong ZX. A novel bio-based epoxy resin from oligomer: Excellent processability, high heat resistance, and intrinsic flame retardancy. Express Polym Lett. 2021;15(12):1189–205. [CrossRef].
22. Afewerki S, Edlund U. Engineering an all-biobased solvent- and styrene-free curable resin. ACS Polym Au. 2023;3(6):447–56. [CrossRef].
23. Trullemans L, Koelewijn SF, Scodeller I, Hendrickx T, Van Puyvelde P, Sels BF. A guide towards safe, functional and renewable BPA alternatives by rational molecular design: Structure–property and structure–toxicity relationships. Polym Chem. 2021;12(41):5870–901. [CrossRef].
24. Yang HS, Cho S, Lee M, Eom Y, Chae HG, Park SA, et al. Preparation of sustainable fibers from isosorbide: Merits over bisphenol—a based polysulfone. Mater Des. 2021;198:109284. [CrossRef].
25. Yue L. Application of bio-based Epoxy Resin as the matrix for composites. In: ACS symposium series. Washington, DC, USA: American Chemical Society; 2018. p. 253–63. [CrossRef].
26. Li X, Lin H, Jiang H, Zhang Y, Liu B, Sun Y, et al. Preparation and properties of a new bio-based epoxy resin/diatomite composite. Polym Degrad Stab. 2021;187:109541. [CrossRef].
27. Memon H, Liu H, Rashid MA, Chen L, Jiang Q, Zhang L, et al. Vanillin-based epoxy vitrimer with high performance and closed-loop recyclability. Macromolecules. 2020;53(2):621–30. [CrossRef].
28. Zhou Z, Su X, Liu J, Liu R. Synthesis of vanillin-based polyimine vitrimers with excellent reprocessability, fast chemical degradability, and adhesion. ACS Appl Polym Mater. 2020;2(12):5716–25. [CrossRef].
29. Zhao Y, Zhang Y, Bai X, Wang Y, Hou W, Huang Y. Catalyst-free and sustainable bio-based epoxy vitrimer prepared based on ester exchange and imine bonding. J Polym Environ. 2024;32(10):4912–24. [CrossRef].
30. Cuevas-Suárez C, Ortiz-Rodríguez L, Alonso-Hernández C. Rosi performance from *Pinus* resin. In: Biofilms based on forest resin for preservation of saladette tomatoes. Ciudad de México, Mexico: ECORFAN; 2024. p. 36–44. [CrossRef].
31. Deng L, Wang Z, Qu B, Liu Y, Qiu W, Qi S. A comparative study on the properties of rosin-based epoxy resins with different flexible chains. Polymers. 2023;15(21):4246. [CrossRef].
32. Hao C, Liu T, Zhang S, Liu W, Shan Y, Zhang J. Triethanolamine-mediated covalent adaptable epoxy network: Excellent mechanical properties, fast repairing, and easy recycling. Macromolecules. 2020;53(8):3110–8. [CrossRef].
33. Chen Q, Wu R, Schott D, Jovanova J. Programmable structure with shape memory materials for soft robotics. Smart Mater Struct. 2026;35(1):015049. [CrossRef].
34. Yang X, Guo L, Xu X, Shang S, Liu H. A fully bio-based epoxy vitrimer: Self-healing, triple-shape memory and reprocessing triggered by dynamic covalent bond exchange. Mater Des. 2020;186:108248. [CrossRef].
35. Zhou J, Jiang G, Wang M, Sun L, Yu H, Zhao D. Biodegradable, thermally stable, and programmable cellulosic bioplastics enabled by supramolecular stimulated mediation. Research. 2026;9:1098. [CrossRef].